

The 3'-modified antisense oligos promote faster hydrolysis of the target RNA by RNase H than the natural counterpart

Edouard Zamaratski, Dimitri Ossipov, P. I. Pradeepkumar, Nariman Amirkhanov
and Jyoti Chattopadhyaya*

Department of Bioorganic Chemistry, Box 581, Biomedical Center, University of Uppsala, S-751 23 Uppsala, Sweden

Received 24 July 2000; revised 5 October 2000; accepted 26 October 2000

Abstract—We have examined the antisense potency of the hybrid duplexes of fully-matched 3', 5' and interior-chromophore tethered antisense oligos (AON) and three target RNAs (11mer and two 17mers) against RNase H, and found them to be better substrates compared to the native DNA/RNA hybrid. These target RNAs were chosen for complexation with AONs because they have very different folding characteristics as evident from the temperature- and concentration-dependent UV and CD spectroscopy. The differences in the tertiary structures of the target RNAs have been exploited here to investigate the kinetic availability of the single-stranded region accessible for the complexation with the AON during the RNase H promoted cleavage. It has emerged that the cleavage rate of the target RNA in the hybrid is independent of the complexity of the folding of the target RNA, thereby suggesting that (i) The kinetic accessibility of the single strand region in all three RNA targets, (11), (12) and (13), by AONs are very similar, and indeed not rate-limiting, although sequence specificities are non-identical in the 11mer and 17mers RNAs. (ii) The rate of conversion of the folded RNA structures to the single-stranded form, and subsequently its kinetic accessibility to drive the hybrid AON/RNA duplex formation is much faster than the RNase H promoted cleavage rate of the RNA moiety in the hybrid. (iii) This also means that the RNase H promoted cleavage rate of the hybrid is the slowest (i.e. the rate-determining). © 2001 Elsevier Science Ltd. All rights reserved.

1. Introduction

Antisense oligonucleotides (AON) exert biological activity by multiple mechanisms of action providing a potentially important tool for the treatment of viral infections, cancer and a number of other diseases.¹ One of the mechanisms involves recruitment of the RNase H for sequence-specific degradation of the target mRNA upon binding to the complementary AON in a catalytic manner. In vivo, RNase H is involved in DNA replication and may play other roles in the cell and it is found in the cytoplasm as well as in the nucleus.²

2'-Deoxyphosphorothioates (PS), the first generation of AON in clinical trial,¹ possess higher nuclease resistance compared to the phosphodiester oligonucleotides (PO) and activate RNase H to cleave the target RNA. Nevertheless PS-AONs have a few major drawbacks: (i) The stability of the RNA/DNA duplexes decreases by 0.5–1°C with introduction of each PS linkage, resulting in poor duplex formation at low AON concentrations. (ii) Administration of higher concentrations or use of a longer PS-AONs can cause negative side effects, including inhibition of RNase H, because of their potency for non-specific binding to proteins.³

In pursuit of improved binding affinity of AONs, modified internucleot(s)ide linkers, heterocyclic bases, or sugar moieties have been introduced: Different 2'-O-alkyl⁴ and 2'-O-aminoalkyl^{1,5} as well as 2'-fluoro⁶ modifications in ribose resulted in significant increases of the duplex stability (about 2°C per modification) and locked nucleic acids (LNA) demonstrated an unprecedented ΔT_m of 46°C for a 9 base-pair long DNA-LNA duplex relative to native DNA/RNA hybrid.⁷ Unfortunately all these modifications drive the sugar into the C3'-endo conformation typical for the A-type RNA/RNA duplex⁸ which results in complete loss of the RNase H activity. However, arabinonucleic acids (ANA) and 2'-deoxy-2'-fluoro-arabinonucleic acids (2'F-ANA) were shown⁹ to be the substrates for RNase H. RNase H activity of the duplexes formed by 2'F-ANA was comparable with the corresponding non-modified substrates, and lower activity observed for ANA/RNA duplexes was attributed to their lower thermodynamic stability.⁹ AONs possessing various 4'-C and 5'-C modifications in 2'-deoxyribose moiety have been reported to serve as substrates for RNase H with efficiency comparable with those of the non-modified DNAs irrespective of their lower affinity to the RNA target.^{10a,b} Morpholino-oligonucleotides, AONs consisting of α -nucleotides, HNA as well as PNA although exhibiting strong binding ability towards RNA are however not found to be suitable substrates for RNase H.^{11a-d} Among various backbone modifications only phosphorothioates^{12a,b} and boranophosphates¹³ were shown to support RNase H hydrolysis.

Keywords: antisense; oligos; RNAs.

* Corresponding author. Tel.: +4618-471-4577; fax: +4618-554495;
e-mail: jyoti@bioorgchem.uu.se

Antisense DNA oligonucleotides (AON):

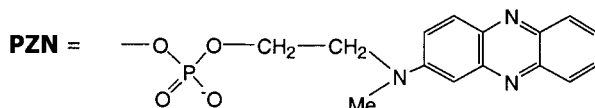
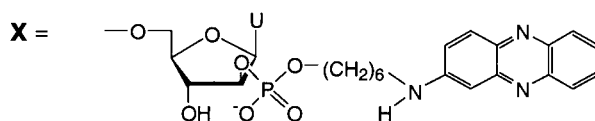
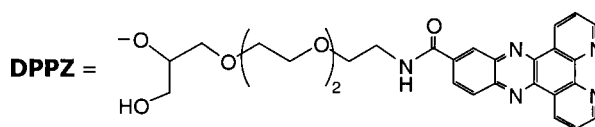
- Phosphodiester backbone (PO):
- (1): 5'-TCCAAACAT-3'
- (2): PZN-5'-TCCAAACAT-3'
- (3): DPPZ-p-5'-TCCAAACAT-3'
- (4): 5'-TCCAAACAX-3'
- (5): 5'-TCCAAACAT-3'-DPPZ

- Phosphorothioate backbone (PS):
- (6): 5'-TsCsCsAsAsAsCsAsT-3'
- (7): PZN-5'-TsCsCsAsAsAsCsAsT-3'
- (8): DPPZ-p-5'-TsCsCsAsAsAsCsAsT-3'
- (9): 5'-TsCsCsAsAsAsCsAsX-3'
- (10): 5'-TsCsCsAsAsAsCsAsT-3'-DPPZ

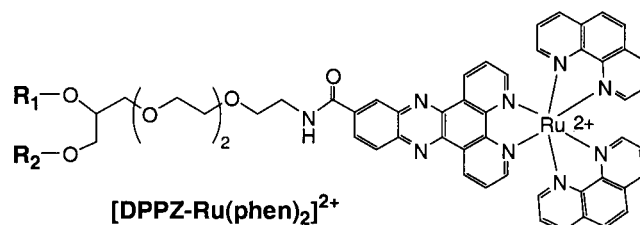
RNA targets:

- (11): 5'-r(CAUGUUUGGAC)-3' (non-aggregated)
- (12): 5'-r(ACUCAUGUUUGGACUCU)-3' (low-aggregated)
- (13): 5'-r(UACAUGUUUGGACUCU)-3' (highly-aggregated)

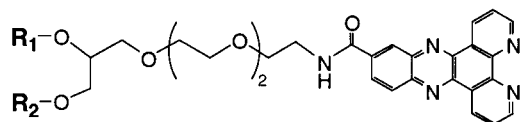
Where:



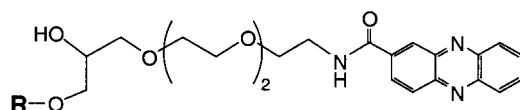
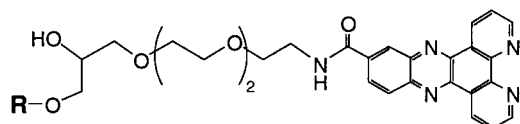
- (14): R₁ = H
R₂ = 5'-TCCAAACAT-3'-p-
- (15): R₁ = -p-5'-TCCAAACAT-3'
R₂ = H
- (16): R₁ = -p-AACAT-3'
R₂ = -p-ACCT-5'



- (17): R₁ = -p-AACAT-3'
R₂ = -p-ACCT-5'



- (18): R = 5'-AGTCCAAACATGA-3'-p-
- (19): R = 5'-AsGsTsCsCsAsAsAsCsAsTsGsA-3'-p-
- (20): 5'-AGTCCAAACATGA-3'
- (21): 5'-AsGsTsCsCsAsAsAsCsAsTsGsA-3'
- (22): R = 5'-AGTCCAAACATGA-3'-p-
- (23): R = 5'-AsGsTsCsCsAsAsAsCsAsTsGsA-3'-p-



- (24): 5'-TACAAACCT-3'-O-P(=O)(OH)-NH-CH₂-CH₂-CH₂-NH-
- (25): 5'-TACAAACCT-3'-O-P(=O)(OH)-NH-CH₂-CH₂-CH₂-NH-

Figure 1. Various AONs and their RNA targets.

Other modifications like methylphosphonates,^{14a,b} phosphoro-*N*-morpholides, phosphoro-*N*-butylamides,¹⁵ formacetals, 3'-thioformacetals,¹⁶ methylenemethyl-imines¹⁷ and N3'→P5' phosphoramidates¹⁸ did not elicit RNase H activity. The high affinity of the above AONs towards

RNA could still be exploited. The first approach arises from the RNase H-independent mechanism of action of AONs.¹ If strongly bound to the target RNA such AON can interfere with metabolic processes associated with the mRNA (translation arrest). The second approach¹ resulted

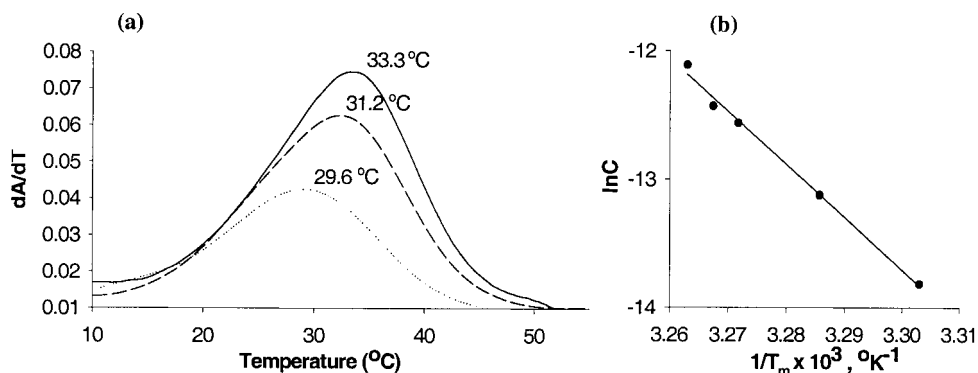


Figure 2. (a) Melting temperature of the RNA/RNA duplex formed by highly-aggregated 17mer RNA (**13**) at: (·····) 1 μ M, (---) 3 μ M and (—) 5 μ M RNA concentration. (b) The plot of $1/T_m$ vs $\ln C$ giving ΔH° and ΔS° parameters from the slope and intercept of fitted line: $1/T_m = (R/\Delta H^\circ) \ln C + \Delta S^\circ/\Delta H^\circ$.

in the appearance of the second generation of AONs-chimeric oligonucleotides with terminals consisting of modified nucleotides to provide high affinity towards target RNA and high nuclease resistance, and the central part of the oligo (PO or PS-backbone) to support RNase H cleavage.^{19a-c} Oligonucleotides containing deoxyuridine and deoxycytidine nucleosides bearing propyne, butyne or dimethylthiazole moieties²⁰ at C5 as well as the recently reported 9-(aminoethoxy)phenoxazine analogue of cytosine (G-clamp)²¹ showed enhanced binding affinity towards RNA but did not improve the ability to recruit RNase H compared to non-modified antisense oligo-DNAs.

Gene-selective, mismatch sensitive and RNase H-dependent inhibition of SV40 large T antigene was reported for PS-AONs as short as heptamers.²² In mammalian cells, an 11mer AON²³ could identify and bind to a unique RNA sequence. We have earlier shown²⁴ that the 5'-tethered chromophore to the 9mer AON leads to a considerable increase of the AON/RNA hybrid stability and, judging from the similarities of their CD spectra with that of the native counterpart, it is clear that the helicity of these AON/RNA duplexes is identical to the native counterpart. This was confirmed by that fact that some of these 5'-tethered AONs already showed enhanced RNase H recruitment compared with the native counterpart. We here report the effect of 3'-phenazine (PZN) and dipyridophenazine (DPPZ) tethers on the RNase H dependent antisense properties of AONs with PO and PS backbones, and compare them with the 5'-counterparts against three different RNA targets, having varying degrees of folded structures. Here we also report the resistance of our 3'-modified AONs towards 3'-exonucleases using snake venom phosphodiesterase.

Interestingly, such 3'-modifications show all the desirable properties for an ideal AON compared to the native counterpart: (i) higher nuclease resistance, (ii) higher capability of stabilizing the resulting AON/RNA duplex, even with short antisense sequence, and (iii) higher RNase H competency.

2. Results and discussion

Native and modified 9mer AONs (**1**)–(**10**) as well as the target RNAs (**11**)–(**13**) were synthesized and purified as

reported earlier (Fig. 1).^{25,26} Each set consists of non-tethered oligonucleotide, two pairs of AONs conjugated either with PZN or DPPZ at the 3'- or 5'-end. The 5'-PZN moiety in AONs (**2**) and (**7**) was tethered through the terminal 5'-phosphate using the aminoethylene linker (Fig. 1). For the 3'-end modification with PZN, *ara*-U moiety was inserted instead of the terminal thymidine where PZN was attached to the 2'-phosphate of *ara*-U using *n*-hexylamino linker (as in AONs (**4**) and (**9**) in Fig. 1). The DPPZ moiety was conjugated to the oligonucleotides through the phosphate using a glycerol moiety extended with a triethylene-glycol linker (as in AONs (**3**), (**5**), (**8**), (**10**), and (**14**)–(**19**), in Fig. 1). The AONs (**1**)–(**10**) were hybridized with complementary 11mer RNA target (**11**). Thermodynamic parameters of these AON/RNA duplexes were extracted from the UV melting experiments²⁷ at different concentrations. CD spectroscopy of the AON/RNA hybrid duplexes was used for conformational characterization according to their resemblance to DNA/DNA, DNA/RNA or RNA/RNA type in comparison with the authentic natural counterpart.²⁸ In order to correlate the stability and structural features of the DNA/RNA hybrids formed by our AONs with their ability to recruit the RNase H, the hybrids were incubated with the enzyme and the extent of hydrolysis and the cleavage patterns were determined by PAGE. The resistance of our 3'-modified AONs against cellular nucleases were assessed²⁹ by incubation with snake venom phosphodiesterase. To evaluate how the tertiary structures of the target RNA^{30a-c} affect the binding to our AONs, we have chosen one 11mer RNA (**11**) and two longer 17mer RNA targets (**12**) and (**13**) with different self-folding capacities. The self-aggregation of these RNA targets was examined by temperature-dependent CD experiments and by UV thermal denaturation studies.

2.1. UV and CD studies of the RNA targets and their self-aggregation in aqueous solution

An oligo-RNA, depending upon the size/length and the specific sequence, is known to form various structural motifs (duplex, triplex, hairpin, pseudoknots etc), resulting from either intramolecular or intermolecular self-assembly processes primarily owing to the various forms of hydrogen-bonding possible between the donor and the acceptor aglycones. Thus the ability of an AON to form a stable duplex with a target RNA depends upon the free-energy

Table 1. Thermodynamic parameters of the self-aggregation of the highly-aggregated 17mer RNA target (**13**) as calculated from the concentration dependent UV melting experiments^a

T_m (°C) ^a	ΔH° (kJ mol ⁻¹)	ΔS° (eu)	ΔG°_{298} (kJ mol ⁻¹)	$-T\Delta S^\circ$ (kJ mol ⁻¹)
29.6	-342.3 (± 25.4)	-1.0 (± 0.08)	-38.3 (± 2.0)	-303.9

^a T_m reported for 1 μ M RNA concentration.

of stabilization of the folded RNA structure by itself compared to the free-energy of stabilization of AON/RNA duplex. Hence, the kinetic accessibility of the target RNA^{30c} by the AON to form a stable structure is an essential prerequisite for the AON/RNA duplex formation to arrest the translation or to activate the RNase H.

Thermal denaturation studies with the 11mer RNA (**11**) at 1 and 5 μ M concentrations showed the absence of any structural transition for this target. Melting experiments with low-aggregated 17mer RNA (**12**) did not show a clear sigmoidal transition although some hyperchromic effect was observed. In contrast, typical monophasic melting

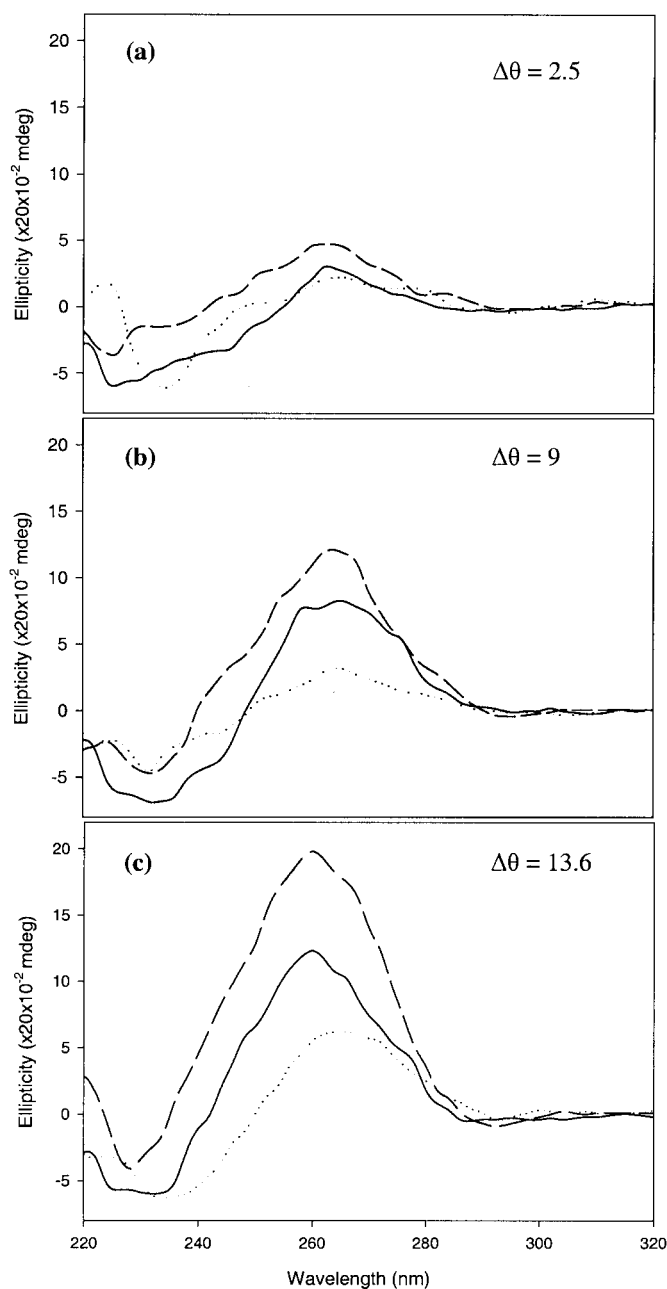


Figure 3. Temperature dependent CD spectra of (a) 11mer RNA (**11**), (b) low-aggregated 17mer RNA (**12**) and (c) highly-aggregated 17mer RNA (**13**) targets at (---) 6°C, (—) 20°C and (.....) 50°C. The extent of the RNA folding is reflected in the value of $\Delta\theta$ (in 20×10^{-2} m²), which is calculated as $\theta_{6^\circ\text{C}} - \theta_{50^\circ\text{C}}$.

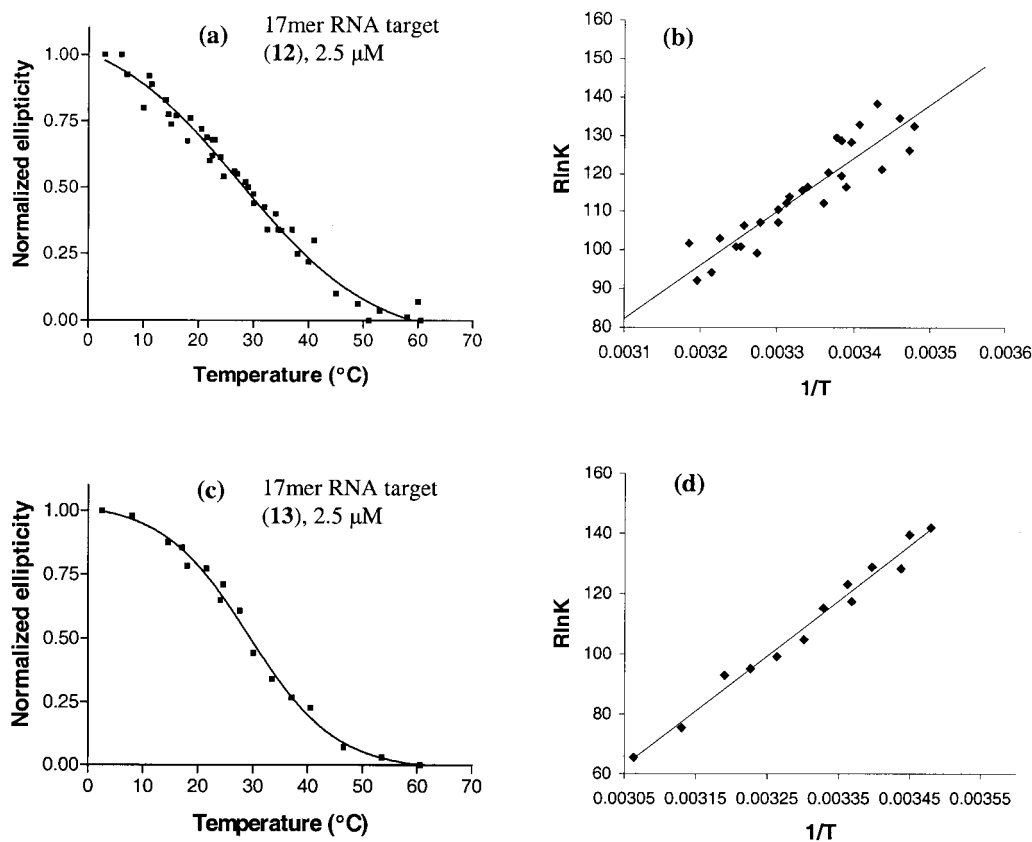


Figure 4. Curves (a) and (c) are typical melting curves for the low- (**12**) and highly-aggregated (**13**) RNA targets, respectively, obtained by fitting the sigmoidal function with variable slopes into the ellipticity vs temperature plots. Curves (b) and (d) are plots of $R\ln K$ vs $1/T$ obtained from the corresponding melting curves, giving the enthalpy, ΔH° , and entropy, ΔS° , from the slope and intercept, respectively: $R\ln K = -\Delta H^\circ/T + \Delta S^\circ$. Equilibrium constants K for each temperature point were calculated as $K = f/2(1-f)^2 C_1$ where f is a fraction of duplex and C_1 is the total strand concentration.

behavior was observed for the highly-aggregated 17mer RNA (**13**) (Fig. 2), which was found to be concentration dependent, and allowed us to calculate the thermodynamics (Table 1) of its self-aggregation process. CD was employed to confirm the tertiary structure formation of the RNA targets. This was particularly valuable in the case of low-aggregated 17mer RNA (**12**), which failed to show any clear transition in the UV melting experiments. The CD spectra of all three RNA targets (**11**)–(**13**) were recorded at three different temperatures. Nucleic acid ellipticity is modulated by disorientation (melting) or reorientation (formation of structural forms) of nucleic acid chromophores.³¹ Thus it can be used for qualitative justification of the extent of the structural assembly and self-organization. Fig. 3a shows that the ellipticity of the 11mer RNA target (**11**) remains almost unchanged upon heating, suggesting a near absence of any significant tertiary structure. This was also evident from the UV thermal denaturation studies, thereby allowing us to conclude that this target does not aggregate to any notable degree in solution. The ellipticity of the highly-aggregated

RNA target (**13**) displayed very strong temperature dependency (Fig. 3c), suggesting a high degree of structural organization. Although the low-aggregated 17mer RNA (**12**) did not show any clear transition in the UV melting experiments, it did, however, exhibit a definite but less pronounced (compared to **13**) temperature dependency of ellipticity (Fig. 3b). Consistent with the earlier observation,³² temperature dependent CD has also been found in this work to be a more sensitive tool to monitor structural transitions in nucleic acids than the UV. Clear temperature and concentration-dependent change of ellipticities at 265 nm were observed for both low- and high-aggregated 17mer RNA targets (**12**) and (**13**) (Fig. 4a and c) by CD, but not for 11mer RNA (**11**). At 1 and 2.5 μM RNA concentrations, the T_m values were found to be 24.7 and 27.7°C for the target (**12**), and 28.8 and 29.8°C for the target (**13**), showing that the self-aggregation process to form RNA/RNA duplexes in solution by these target RNAs indeed results from the bimolecular interstrand interactions (Fig. 5). The thermodynamic parameters of duplex formation

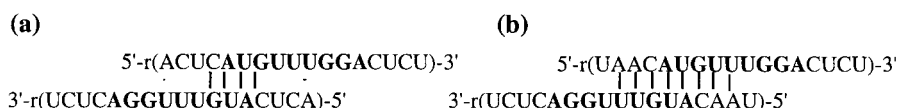


Figure 5. Proposed structures of RNA/RNA duplexes formed by (a) low-aggregated 17mer RNA target (**12**) and (b) highly-aggregated 17mer RNA target (**13**), resulting from intermolecular self-aggregation in solution. Bold letters represent the sequence complementary to the antisense DNAs.

Table 2. Thermodynamics of RNA/RNA duplex formation for the low- and highly-aggregated RNA targets (**12**) and (**13**) calculated from CD melting curves

RNA target	T_m^a (°C)	ΔH° (kJ mol ⁻¹)	ΔS° (eu)	$-T\Delta S^\circ$ (kJ mol ⁻¹)	ΔG_{298}° (kJ mol ⁻¹)
(12)	27.7	-139	-0.35	104.3	-34.7
(13)	29.8	-200	-0.54	160.9	-39.1

^a The T_m s are shown for 2.5 μ M RNA concentration.

for the both low- and high-aggregated 17mer RNA targets (**12**) and (**13**) from the temperature dependent CD measurements are shown in Table 2.

2.2. UV Melting and thermodynamic studies on the DNA/RNA hybrids

2.2.1. Studies with the non-aggregated 11mer RNA target (11). All chromophore-conjugated (both PO and PS) AON/RNA duplexes demonstrated higher stability compared to the non-conjugated counterparts, which was evident from the magnitude of T_m and the free-energy change (ΔG_{298}°). In all these cases the value of pairing entropy (ΔS°), which is a measure of the conformational constraints of the oligo chain, was found to be higher than that for non-modified duplexes (Tables 3 and 4). This can be attributed to the effect of the conformationally flexible tethers employed for the chromophore attachment. On the other hand, the additional π - π stacking between aromatic rings of the chromophore and base-pairs of the duplex provides a significant gain in enthalpy (ΔH°). This clearly indicates the strong enthalpy assistance to the duplex formation by the DPPZ and PZN tethered ODNs with the complementary RNA. The 3'-modifications with both PZN and DPPZ resulted in more stable AON/RNA hybrids as compared to the 5'-counterparts. Among all the duplexes tested, 3'-DPPZ-AON/RNA hybrids were found to be the most stable, which is reflected in the net free energy of stabilization $\Delta\Delta G_{298}^\circ$ of -8.1 kJ/mol for PO and -3.9 kJ/mol for PS oligonucleotides, where $\Delta\Delta G_{298}^\circ$ signifies $[\Delta G_{298}^\circ]_{\text{tethered duplex}} - [\Delta G_{298}^\circ]_{\text{non-tethered duplex}}$. But in the case of 3'-PZN-AONs, $\Delta\Delta G_{298}^\circ$ is reduced to -5.4 kJ/mol (PO) and 1.75 kJ/mol (PS), showing the better stacking capability of the DPPZ group compared to the PZN when it is attached to the 3'-end of oligonucleotide. When the DPPZ group is tethered at the 5'-end, the net free energy of duplex stabilization is lower ($\Delta\Delta G_{298}^\circ =$

-4.9 kJ/mol for PO-oligo and -1.0 kJ/mol for PS-oligo) compared to the 5'-PZN-AONs ($\Delta\Delta G_{298}^\circ = -6.0$ kJ/mol (PO) and -1.4 kJ/mol (PS)).

2.2.2. Studies with the low-(12) and highly-(13) aggregated 17mer RNA targets. When the low-aggregated 17mer RNA target (**12**) was hybridized with the 9mer AONs (**1**)–(**5**), clear helix-to-coil transitions were observed. All duplexes formed by modified AONs (**2**)–(**5**) with the low-aggregated 17mer RNA target (**12**) had T_m values very close to those of duplexes formed with the 11mer RNA target (**11**) (Table 5). The T_m of the duplex formed by the native AON (**1**) and the low-aggregated 17mer RNA target (**12**) was 2°C lower compared to that with the 11mer RNA target (**11**). The T_m s of the duplexes formed by the tethered thio-AONs (**7**)–(**10**) and the low-aggregated 17mer RNA target (**12**) were somewhat lower compared to the T_m s of the corresponding duplexes with the 11mer RNA (**11**). No distinct transition was observed with the blank thio-AON (**6**) and the low-aggregated 17mer RNA target (**12**). The hybrids of the thio-AONs (**6**)–(**10**) and the native AON (**1**) with 11mer RNA (**11**) have lower ΔG_{298}° of duplex formation (between 29.5 and 33.8 kJ/mol) compared to ΔG_{298}° of the self-aggregation process in the 17mer RNA target (**12**) (34.7 kJ/mol). The free energies of both processes are very close, resulting in two competing structures, i.e. AON/RNA and RNA/RNA duplexes, in comparable concentrations in solution. The duplex formed by the blank thio-AON (**6**) and the 11mer RNA (**11**) had the lowest ΔG_{298}° , and was also not able to compete and interrupt the tertiary structure of the low-aggregated 17mer RNA target (**12**) to form a hybrid duplex structure. This, along with the ΔG_{298}° of the other tethered PS-AON/RNA duplexes (Table 4) shows that the tethered-chromophore thermodynamically assists in the equilibrium shift of the self-aggregation process of the target RNA toward the AON/RNA hybrid duplex formation.

Table 3. The T_m s (1 μ M of AON concentration) and thermodynamic parameters of the duplexes formed by 11mer RNA target (**11**) and PO-AONs (**1**)–(**5**)

AON	T_m (°C)	ΔT_m (°C)	ΔH° (kJ mol ⁻¹)	ΔS° (eu)	$-T\Delta S^\circ$ (kJ mol ⁻¹)	ΔG_{298}° (kJ mol ⁻¹)	$\Delta\Delta G_{298}^\circ$ (kJ mol ⁻¹)
(1)	22.1	–	-226±8	-0.65±0.03	192.2	-33.8±0.5	–
(2)	28.7	6.5	-298±4.5	-0.87±0.01	258.0	-39.8±0.1	6
(3)	27.6	5.5	-286±20	-0.83±0.07	248.1	-38.7±2.8	4.9
(4)	28.6	6.5	-256±10	-0.73±0.03	216.8	-39.2±1.5	5.4
(5)	30.6	8.5	-316±23	-0.92±0.07	274.5	-41.9±3.2	8.1

Table 4. The T_m s (1 μ M of AON concentration) and thermodynamic parameters of the duplexes formed by 11mer RNA target (**11**) and PS-AONs (**6**)–(**10**)

AON	T_m (°C)	ΔT_m (°C)	ΔH° (kJ mol ⁻¹)	ΔS° (eu)	$-T\Delta S^\circ$ (kJ mol ⁻¹)	ΔG_{298}° (kJ mol ⁻¹)	$\Delta\Delta G_{298}^\circ$ (kJ mol ⁻¹)
(6)	16.6	–	-220±14	-0.64±0.05	190.5	-29.5±1.6	–
(7)	19.1	2.4	-245±20	-0.72±0.06	214.0	-30.9±2.7	1.4
(8)	19.3	2.7	-279±14	-0.83±0.05	248.7	-30.6±1.3	1.1
(9)	19.7	3.1	-267±3.5	-0.79±0.01	236.1	-31.3±0.6	1.8
(10)	22.0	5.3	-257±15	-0.75±0.05	223.5	-33.4±1.5	3.9

Table 5. The T_m s ($^{\circ}\text{C}$, 1 μM of AON concentration) observed when low-aggregated 17mer RNA target (**12**) and highly-aggregated 17mer RNA target (**13**) were hybridized with AONs (**1**)–(**10**)

Oligos	(1)	(2)	(3)	(4)	(5)	(6)	(7)	(8)	(9)	(10)
(12)	20.2	28.5	27.7	28.1	30.7	11–14 ^a	15.7	18.2	15.9	20.9
(13)	28.6	30.5	29.2	30.4	30.3	29.3	28.9	29.1	29.2	29.2

^a Very broad transition

When AONs were hybridized with highly-aggregated 17mer RNA target (**13**), all the T_m s observed by UV were close to the T_m of the target itself (Tables 1 and 5), which made it impossible to estimate the extent of the AON/RNA duplex formation. This can be explained by comparison of ΔG°_{298} values for the corresponding AON/11merRNA hybrids with the ΔG°_{298} value of the self-aggregation process of the 17mer RNA target (**13**) (Table 1). The free-energies of the duplex formation for all the tethered AONs were comparable (between 38.7–41.9 kJ/mol) with ΔG°_{298}

for the RNA/RNA duplex formation ($\Delta G^{\circ}_{298} = -38.4$ kJ/mol). This means that only a fraction of AON strands was able to form the desirable AON/RNA hybrid, while a considerable portion of the RNA remained in the aggregated state.

2.3. CD Experiments on the DNA/RNA hybrids

To investigate the influence of the tethered chromophores on the global helical conformation of the AON/RNA hybrid duplex, the CD spectra of duplexes formed by AONs (**1**)–(**10**) with the 11mer RNA target (**11**) were recorded at 16 $^{\circ}\text{C}$ under identical condition (see experimental). All modified duplexes exhibited spectra supporting an intermediate structure between A-type RNA/RNA and B type DNA/DNA hybrids, mimicking those of natural DNA/RNA hybrids³³, in which the DNA strand is of the B-type and the RNA strand is of the A-type³⁴. Thus the duplexes formed by AONs (**2**)–(**10**) with 11mer RNA target (**11**) have CD spectra very similar to the blank duplex formed by the

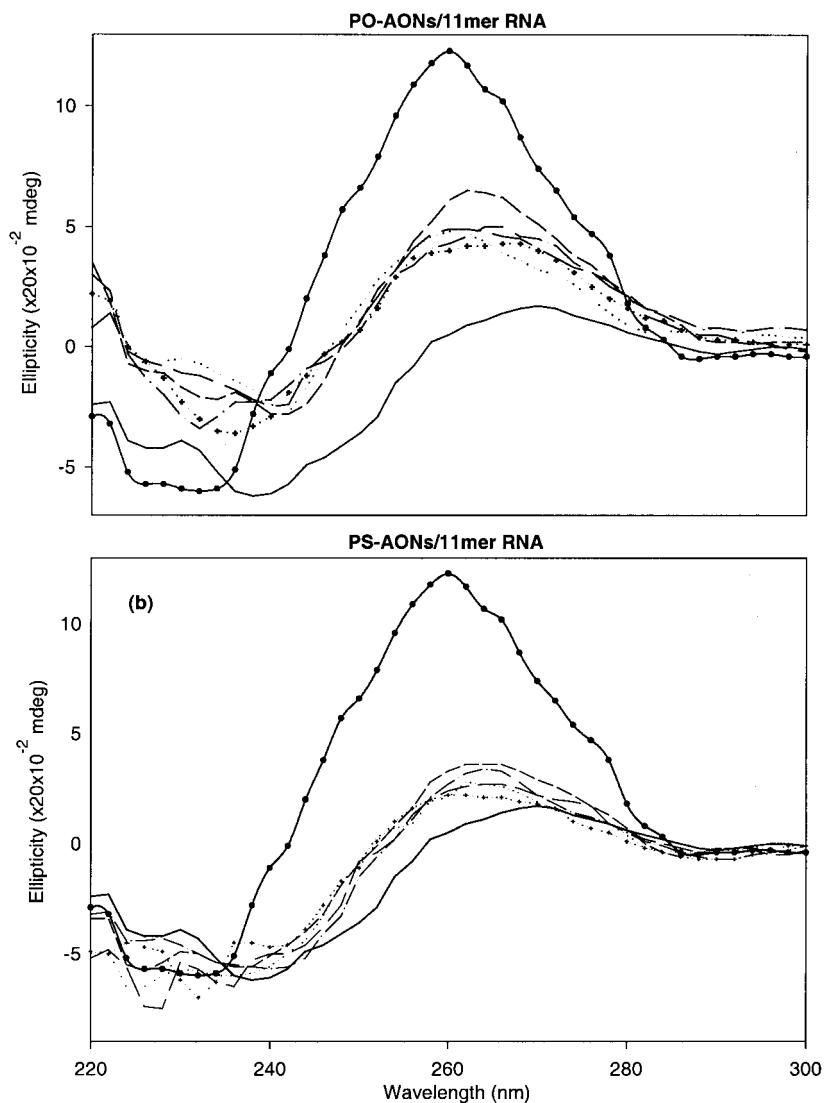


Figure 6. CD spectra of duplexes formed by AONs with 11mer RNA target (**11**) in RNase H digestion buffer at 16 $^{\circ}\text{C}$. (a) PO-AON/RNA hybrids: (---) blank oligo (**1**), (.....) (**2**), (-·-·-) (**3**), (—) (**4**), (----) (**5**). (b) PS-AON/RNA hybrids: (---) blank oligo (**6**), (.....) (**7**), (-·-·-) (**8**), (—) (**9**), (----) (**10**), (—) DNA/DNA (B-type) duplex formed by blank AON (**1**) and complementary 11mer DNA-5'-d(CATGTTTGAC)-3', (-·-·-) RNA/RNA (A-type) duplex formed by the highly-aggregated 17mer RNA (**13**), (see the duplex structure on Fig. 5b).

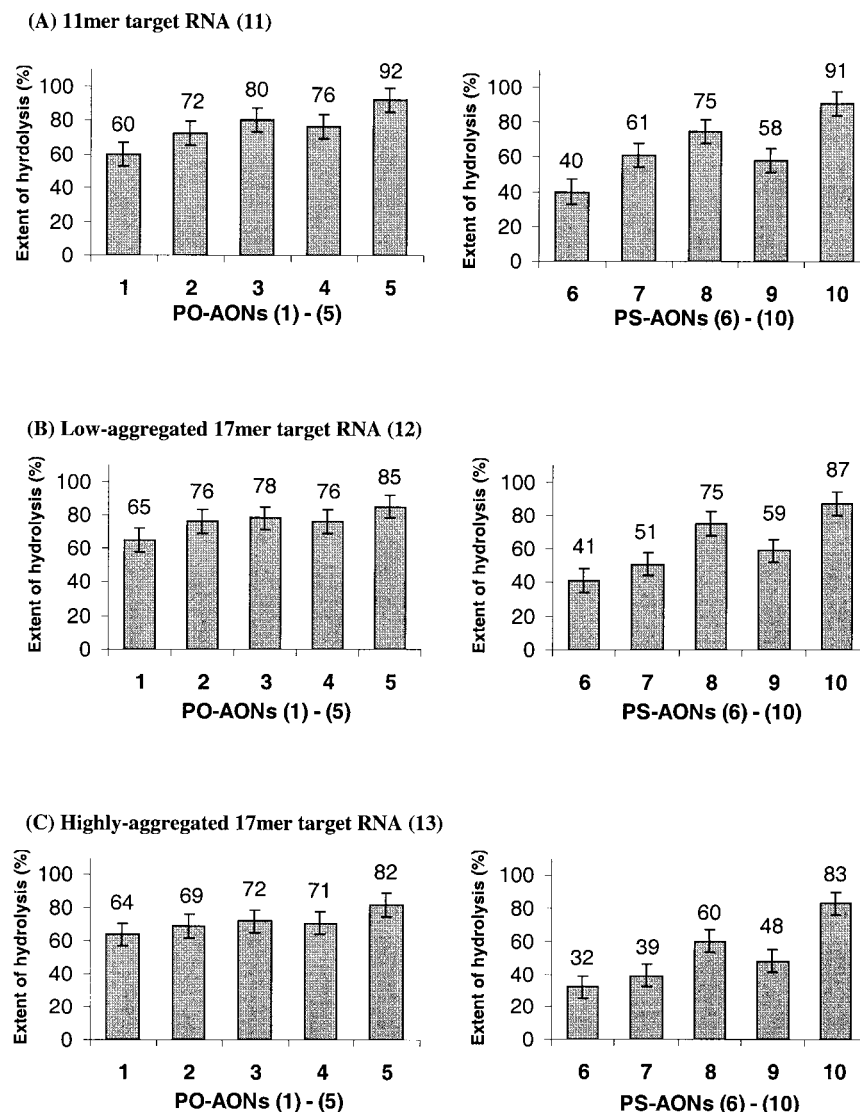


Figure 7. Extent of the PO-AONs (1)–(5) and PS-AONs (6)–(10) promoted RNase H hydrolysis of the (a) 11mer RNA target (11), (b) low-aggregated 17mer RNA (12), (c) highly-aggregated 17mer RNA (13) after 2 h of incubation

native AON (1) and RNA target (11), rather than those of the native DNA/DNA or RNA/RNA duplex (Fig. 6). The spectra of the modified duplexes had a positive band at 260–266 nm, a negative band at 234–240 nm and a crossover point at 247–248 nm (the corresponding parameters for the non-modified duplex were 264, 232 and 248 nm, respectively). Changing the PO-backbone to PS did not alter the global conformation of the AON/RNA duplexes, which is in agreement with previous reports.³⁵ For all tethered PS-AON/RNA duplexes, positive CD bands were observed at 262–265 nm, negative CD bands at 234–240 nm and crossover points at 252–254 nm, which were very close to the corresponding parameters found for the natural hybrid duplex (264, 240 and 254 nm, respectively). These data suggested that neither 3'- nor 5'-modifications altered the global helical structure from a native DNA/RNA hybrid, which suggested to us that the hybrid duplexes formed by the chromophore-tethered AONs have the potential to be as good substrates for RNase H as the natural DNA/RNA hybrids, as was latter demonstrated by RNase H digestion study (see below).

2.4. RNase H digestion studies of the hybrid AON-RNA duplex

2.4.1. With 11mer target RNA (11). RNase H recruitment is an important factor governing the antisense activity of AONs. We examined whether the chromophore-tethered AON/RNA hybrids could elicit RNase H activity. The 5'-³²P labelled 11mer RNA (11) was hybridized with complementary AON strands (see experimental) and incubated with *Escherichia coli* RNase H at 21°C. Aliquots were taken after 15 and 120 min intervals, and analyzed by PAGE; the extent of hydrolysis was estimated from the residual full length RNA left after a given incubation time. All modified PO-AONs (2)–(5) promoted a higher degree of RNA hydrolysis compared to the natural counterpart (1) (Fig. 7). The use of chromophore-tethered AONs allowed us to increase the extent of the cleavage of the target RNA (after 2 h of incubation) to 72–80% and even up to an impressive 92% in the case of 3'-DPPZ-AON (5) compared to 60% hydrolysis of the native DNA/RNA hybrid. This result is in good agreement with the

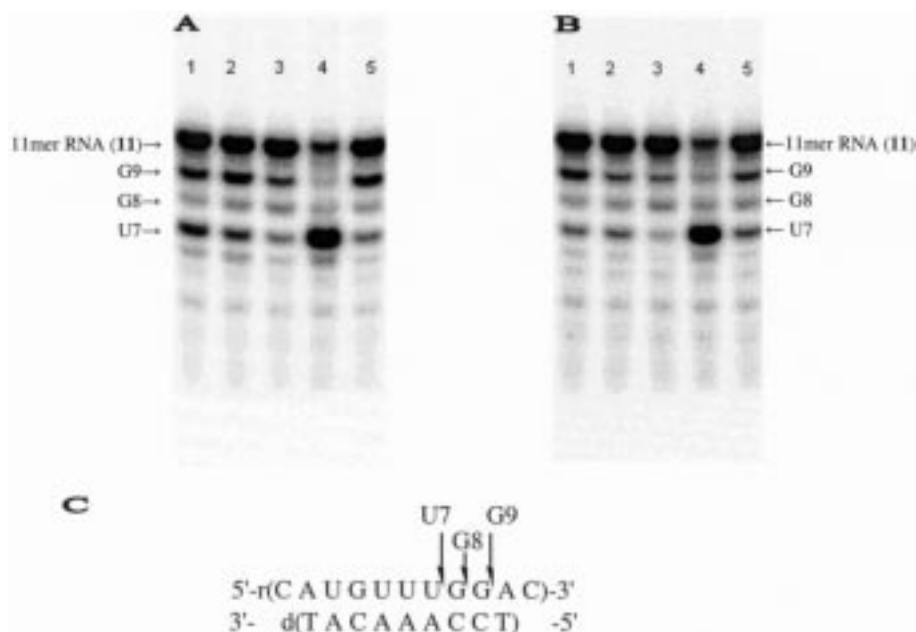


Figure 8. (a) RNase H hydrolysis of 11mer RNA (**11**) after 15 min of incubation when hybridized with PO-AONs: Lanes 1–5 correspond to the reactions with oligos (**3**), (**2**), (**1**), (**5**), (**4**), respectively. (b) RNase H hydrolysis of 11mer RNA (**11**) after 15 min of incubation when hybridized with PS-AONs: Lanes 1–5 correspond to the reactions with oligos (**8**), (**7**), (**6**), (**10**), (**9**), respectively (c) RNase H degradation pattern of 11mer RNA hybridized with modified and native 9mer AONs (**1**)–(**10**). Arrows indicate the major cleavage sites.

thermodynamic stabilities (Table 3) of the corresponding duplexes where all modified AON/RNA hybrids had higher stability compared to the native counterpart. Also noteworthy is the fact that the 3'-DPPZ-modified AON/RNA duplex was the most stable amongst all modified AON/RNA hybrids, and as discussed above, the hydrolysis of RNA strand was also the highest. As evident from the PAGE pictures of the aliquots taken after 15 min of incubation with the enzyme (lane 4 in Fig. 8a), the 3'-DPPZ modified AON (**5**) not only promoted the highest extent of RNA hydrolysis, but also the fastest hydrolysis rate, reaching 83% of the cleaved target RNA compared to 27% for the blank duplex (lane 3 in Fig. 8a) and 35–41% for the other modified substrates (lanes 1, 2, and 5 in Fig. 8a). It is noteworthy that all modified AON/RNA duplexes had the same cleavage sites (Fig. 8c) as the native counterpart. The exception was found for the 3'-DPPZ-conjugated hybrid, which showed site-specific hydrolysis, and had only one single cleavage site at the U7 position (Fig. 8c). The extent of hydrolysis for thio-AON/RNA substrates (AONs (**6**)–(**10**)) (Fig. 8b) was slightly lower compared to the PO analogues as expected from the lower thermodynamic stability of these duplexes. The extent of hydrolysis (2 h of incubation) for the blank PS-AON duplex was 40% and 58–75% for the modified PS-AON duplexes (Fig. 8b).

As in the case of PO-analogues, 3'-DPPZ modification provided the highest degree of digestion (91%) and the highest relative rate of hydrolysis (Fig. 7a). All these data show that the general drawback of thio-AONs (relatively poorer thermodynamic stability of their duplexes with RNA compared to the native counterpart) as antisense drugs can be effectively compensated by tethering a suitable chromophore at the 3' or at the 5'-end of the thio-ANAs (extent of the hydrolysis for blank PO-AON/RNA duplex was 60%, for blank PS-AON/RNA duplex: 40%, and modi-

fied PS-AON/RNA duplexes: 58–91%). Changing the backbone from PO to PS did not alter the cleavage sites for blank as well as for the modified duplexes. For the 3'-DPPZ modified thio-AON/RNA duplex only a single cleavage site was observed at the same position as for PO counterpart (Fig. 8b).

2.4.2. With aggregated 17mer RNA targets (**12**) and (**13**).

The effect of AONs on the cellular target RNAs depends on the choice of complementary target sequence. The tertiary structures of the RNA targets have been shown^{30a-c} to affect the corresponding AON/RNA stability. Usually, the AONs are directed³⁶ at the single-stranded region of the target RNA, lacking any tertiary structure. There is, however, little information available on the RNase H dependent antisense activity of AONs when they are targeted to RNAs having varying degrees of folded structures. This has prompted us to examine the effect of the RNA self-aggregation on the antisense potency of chromophore-tethered AONs. When PO and PS-AONs were hybridized with the low aggregated 17mer RNA (**12**), hydrolysis rates remained approximately the same as those with the non-aggregated 11mer RNA (**11**) (Fig. 7b). In the case of the highly-aggregated 17mer RNA target (**13**) and PO-AONs, we also did not observe any change in the extent of hydrolysis compared to 11mer target RNA (**11**) (Fig. 7c). As it was shown before, PO-AON/RNA hybrids have slightly higher thermodynamic stability than the RNA/RNA duplex formed by the 17mer RNA target (**13**), suggesting that the population of the AON/RNA hybrids is presumably more than that of the intermolecularly aggregated RNA target. This is presumably the reason why the extent of hydrolysis of AON/RNA hybrids was not affected by the tertiary structure of the highly aggregated 17mer RNA target (**13**). The thio-AONs (**6**)–(**10**) were more sensitive to the self-aggregation of the target RNA (Figs 7a and b).

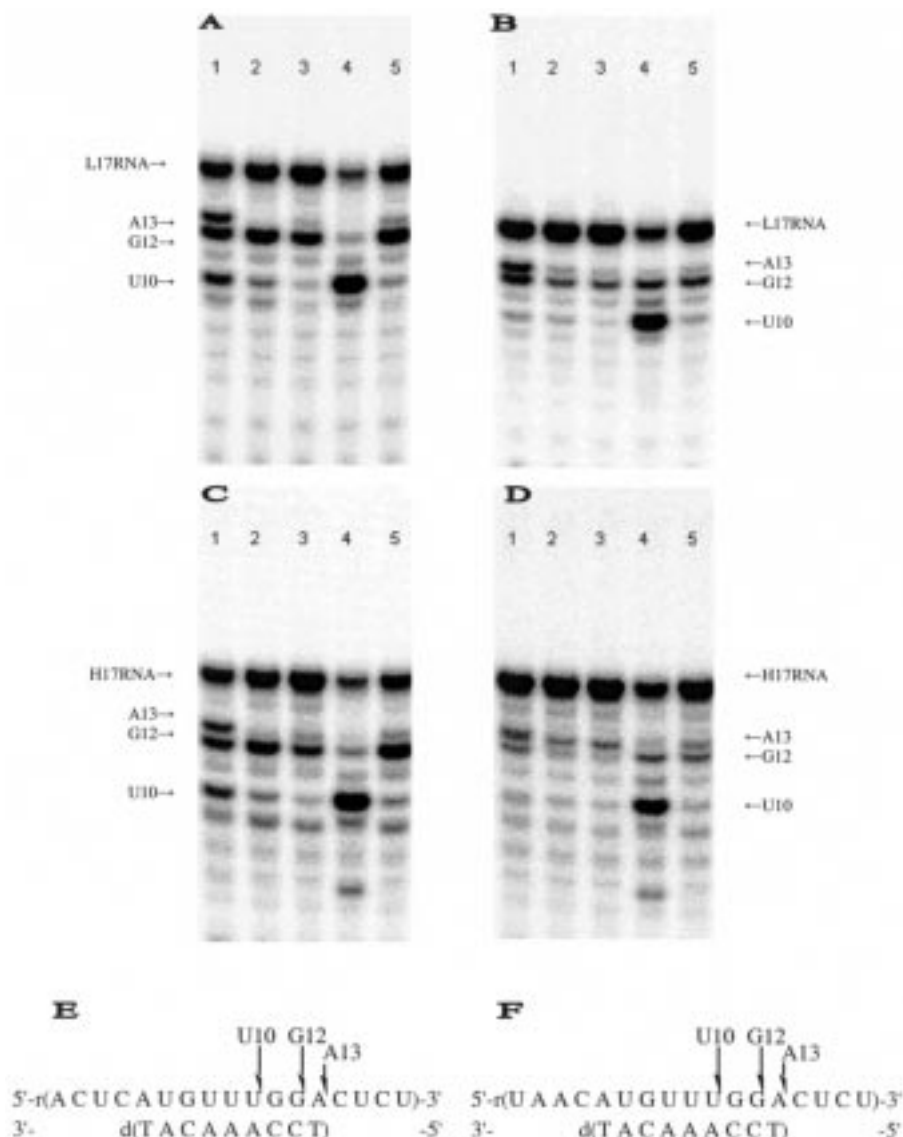


Figure 9. (a) RNase H hydrolysis of low-aggregated 17mer RNA (**12**) hybridized with PO-AONs. (b) RNase H hydrolysis of low-aggregated 17mer RNA (**12**) hybridized with PS-AONs. (c) RNase H hydrolysis of highly-aggregated 17mer RNA (**13**) hybridized with PO-AONs. (d) RNase H hydrolysis of highly-aggregated 17mer RNA (**13**) hybridized with PS-AONs. On each gel picture lanes 1–5 correspond to the reactions with oligos (**3**), (**2**), (**1**), (**5**), (**4**) (PO-AONs) or (**8**), (**7**), (**6**), (**10**), (**9**) (PS-AONs) respectively. RNase H degradation pattern of low- (e) and highly- (f) aggregated 17mer RNA targets hybridized with modified and native 9mer AONs (**1**)–(**10**). Arrows indicate the major cleavage sites.

All thio-AONs promoted poorer hydrolysis with highly-aggregated 17mer RNA target (**13**) compared to the non-aggregated 11mer RNA target (**11**) with the exception of 3'-DPPZ-modified thio-AON (**10**) which forms the most stable AON/RNA duplex. Both aggregated 17mer RNA targets (**12**) and (**13**) had fewer common RNase H cleavage sites in contrast with the short non-aggregated 11mer RNA target (**11**) (Fig. 9e and f) with all AONs: (i) the native as well as 3'- and 5'-PZN-modified duplexes cleaved at the G12 position of the target RNA (**12**) and (**13**), whereas for the 11mer RNA target (**11**), the cleavage sites were U7 and G9 [corresponds to U10 and G12 sites, respectively, in RNA (**12**) and (**13**)] (Fig. 9a–d). (ii) the 3'-DPPZ-tethered PO (**5**) and PS-AON (**10**) promoted a specific cleavage at the U10 position of the RNA targets (**12**) and (**13**), which is the same cleavage site [corresponds to U7 in RNA (**11**)] observed for 11mer RNA target (**11**) (Fig. 8c).

The 5'-DPPZ-modified AONs (**3**) and (**8**) promoted the cleavage of the aggregated 17mer RNA targets at G12 position with one additional A13 cleavage site (Fig. 9a–d). It is noteworthy that on both aggregated RNA targets (**12**) and (**13**) 3'-DPPZ-modification (for both PO and PS-AONs) resulted in an exceptionally high hydrolysis rate as in the case of non-aggregated 11mer RNA target (**11**) as evident from the PAGE pictures on Fig. 9a–d.

The above result shows that given similar nucleobase composition, and different ΔG_{298}° of the self-aggregation but identical AON hybridization sequence, the single strand accessibility of two differently folded 17mer RNAs (**12**) and (**13**) is the same in contrast to the relatively unfolded 11mer RNA target (**11**), where more single strand sites are accessible.

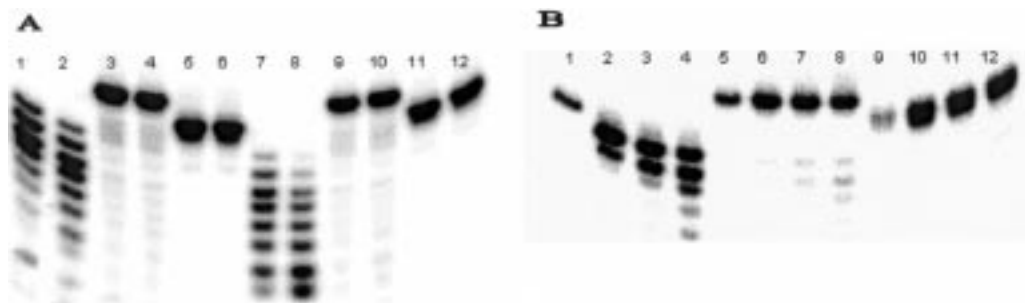


Figure 10. (a) Snake venom PDE degradation of the 3'-PZN- (4) and 3'-DPPZ-modified (5) and native (1) PO-AONs. In lanes 1–6 the concentration of 17.5 ng/ μ l of PDE was used: Lane 1: AON (1), 20 min; lane 2: AON (1), 120 min; lane 3: AON (5), 20 min; lane 4: AON (5), 120 min; lane 5: AON (4), 20 min; lane 6: AON (4), 120 min. Lanes 7–12 represent the same set of the reactions but with double amount of the enzyme (35 ng/ μ l). (b) Snake venom PDE degradation of the 3'-PZN- (9) and 3'-DPPZ-modified (10) and non-modified (6) PS-AONs: Lane 1: AON (6), 0 min; lane 2: AON (6), 10 min; lane 3: AON (6), 30 min; lane 4: AON (6), 120 min; lane 5: AON (10), 0 min; lane 6: AON (10), 10 min; lane 7: AON (10), 30 min; lane 8: AON (10), 120 min; lane 9: AON (9), 0 min; lane 10: AON (9), 10 min; lane 11: AON (9), 30 min; lane 12: AON (9), 120 min.

The fact that all three target RNAs, although each one of them has very different folded structure, are cleaved in the hybrid AON/RNA duplex at a relatively comparable rate, suggests the following: (a) The kinetic accessibility of the single strand region in all three RNA targets, (11), (12) and (13), by AONs is very similar, and indeed *not* rate-limiting, although sequence specificities are non-identical in the 11mer and 17mers RNAs. (b) The rate of conversion of the folded RNA structures to the single-stranded form, and subsequently its kinetic accessibility to drive the hybrid AON/RNA duplex formation is much faster than the RNase promoted cleavage rate of the RNA moiety in the hybrid. (c) This also means that the RNase promoted cleavage rate of the hybrid AON/RNA duplex is the slowest (i.e. the rate-determining).

2.5. Nuclease resistance

AON should also be resistant toward metabolic degradation in plasma.^{37,38} Natural oligonucleotides are very easily degraded by nucleases present in the cells media with half-lives ranging from 10 min to 2 h.³⁹ This makes the *in vivo* fate of AONs an important issue for nucleic acid based therapeutics.

A 3'-exonuclease activity was found to be responsible for most of the oligonucleotide degradation. Modification of AONs at the 3'-end with different lipophilic and aromatic residues helped significantly to minimize the extent of degradation.^{40a,b} To explore the protective properties of 3'-PZN and 3'-DPPZ modifications, AONs (4), (5), (9) and (10) as well as non-tethered PO-AON (1) and PS-AON (6) were incubated with snake venom phosphodiesterase (see Methods for details). Under experimental conditions non-modified PO-AON (1) had a half-life of 4 min, and was almost completely destroyed after 20 min. However, 3'-PZN (4) and 3'-DPPZ (5) PO-AONs did not show any

sign of degradation even after 2 h of incubation (Fig. 10a). A higher concentration of snake venom phosphodiesterase was used in experiments with AONs containing thioate backbone as they are more stable towards exonuclease degradation. The half-life for non-modified PS-AON (6) was 30 min, while that for modified PS-AONs (9) and (10) remained more than 90% intact after 2 h of incubation.

Most probably the steric hindrance caused by the tethered polyaromatic system as well as the flexible linker prevent binding of the enzyme to the oligonucleotide and result in the improved resistance observed with 3'-modified AONs. Interestingly, for both PO and PS-AONs the 3'-PZN modification resulted in approximately 6 times higher stability compared to 3'-DPPZ modifications. This additional resistance shown by 3'-PZN AONs could be attributed to the presence of the unnatural *ara*-U nucleotide at the 3'-end of these oligonucleotides. Arabinonucleic acids¹ were shown to be more nuclease-resistant than native DNA and therefore the 3'-*ara*-U moiety could contribute to the stability of these modified DNAs.

2.6. RNase H sensitivity towards the antisense strand modifications in the hybrid duplex

Structural requirements for the DNA/RNA hybrids to be suitable substrates for RNase H are well described.³³ However the tolerance level of this enzyme towards the modifications, which do not alter the helicity of the duplex is not clearly understood. It is likely that different tethers with various structural parameters (lipophilicity, bulk, presence of charges etc.) should affect the binding affinity of the enzyme to the hybrid duplex and, therefore, the cleavage rates. It was recently reported that AONs conjugated at the 3'-end to the polyethylene glycol moieties of different structure and molecular weight stimulate the

Table 6. Dependency of the extent of RNase H hydrolysis of the low-aggregated 17mer RNA target (12) hybridized with 9mer PO-AONs from the bulk of the modification and the tethering site (the extent of hydrolysis for non-modified oligo (1) was 60%)

Modification at the 3'-end	Extent of hydrolysis	Modification at the 5'-end	Extent of hydrolysis	Modification in the middle	Extent of hydrolysis
DPPZ (5)	91%	DPPZ (3)	75%	DPPZ (17)	50%
Ru-complex (14)	92%	Ru-complex (15)	49%	Ru-complex (16)	4%

hydrolysis of RNA by RNase H at the same sites and to the same extent as the native oligo-DNA.⁴¹

Our studies showed that various tethers at the 3'-end of AON can be very easily tolerated by the enzyme. The DPPZ is more bulky than PZN moiety, but when attached to the 3'-end of AON it provided higher RNase H activity of the corresponding AON/RNA duplexes. Even when 3'-DPPZ moiety in (**5**) was substituted with more bulky and non-planar 3'-[DPPZ-Ru(phen)₂]²⁺ complex (**14**) (Fig. 1) the extent of the RNase H cleavage was not diminished (Table 6), and, in fact, remained much higher than for the native counterpart. This change of the steric and electronic properties of the 3'-group did not have any influence on the cleavage pattern, revealing the same single site of cleavage as for the 3'-DPPZ-AON (**5**). The effect of charge brought by the [DPPZ-Ru(phen)₂]²⁺ complex in (**14**) should also be taken in consideration.

In order to investigate the effect of the positive charge of the tethered ligand at the 3'-end of the AON without seriously altering of the size of the tether, we have compared the extent of cleavage promoted by 3'-phenazinium-AON (**24**) and 3'-phenazine-AON (**25**) (Fig. 1): These modifications have almost the same size, but the phenazinium moiety possesses a positive charge because of the nitrogen alkylation at the N9 position. When such AONs were hybridized with the 17mer RNA target (**12**), the extent of RNase H mediated hydrolysis was found to be the same and very similar to that found for 3'-PZN AON (**4**). These results clearly show that neither of such factors as steric bulk or charge of the modification located at the 3'-end of AON can interfere with RNase promoted cleavage.

In contrast, the 5'-end of AON was more sensitive to the steric bulk of the tether. Substitution of the 5'-DPPZ moiety in AON (**3**) with 5'-[DPPZ-Ru(phen)₂]²⁺ complex (AON (**15**) in Fig. 1) dramatically reduced the extent of the cleavage (49%) to a level which was even poorer than for the native hybrid (60%). In our examples, the cleavage of the target RNA in the AON/RNA duplex takes place at the sites opposite to the 5'-end of the AON segment, and presence of any tether at this position (especially as large as [DPPZ-Ru(phen)₂]²⁺ complex) might interfere with the cleavage. This could be the reason why relatively small intercalators like PZN or DPPZ were tolerated at the 5'-end by the enzyme but not the [DPPZ-Ru(phen)₂]²⁺-modification.

When DPPZ or [DPPZ-Ru(phen)₂]²⁺ modifications were introduced in the middle (AONs (**17**) and (**16**) respectively in Fig. 1) of the duplex formed by 11mer RNA target no hydrolysis by RNase H was observed. When these centre-modified AONs (**16**) and (**17**) were targeted to the low-aggregated 17mer RNA target (**12**) hydrolysis with DPPZ modification (**17**) was observed although to the less extent compared to the native AON-RNA duplex (Table 6), but no significant hydrolysis was achieved with centre-[DPPZ-Ru(phen)₂]²⁺-modified AON (**16**) (Table 6). As an endonuclease RNase H is supposed to bind within the DNA/RNA hybrid before any cleavage can take place. Presumably our modifications placed in the middle prevent the enzyme from binding which results in poorer or even complete loss of RNase H activity of such AONs.

3. Conclusions

1. Thermodynamic properties of the AON/RNA hybrids are improved by tethering aromatic chromophores at the 3'- or at the 5'-ends.
2. Although the thermodynamic stabilities are improved by tethering of aromatic chromophores at the terminus, the interior helical structure remain unaltered as evident by CD.
3. The extent of RNase promoted hydrolysis is improved compared with the native DNA/RNA counterpart.
4. The nature of intercalator/chromophore not only influences the rate of hydrolysis but dictates the cleavage pattern as well. Thus, all PZN-modified 9mer AONs (**2**, **4**, **7**, **9**) share the same cleavage sites with non-modified AON (**1**) on all RNA targets. However, 3'-DPPZ modified AONs (**5**) and (**10**) promoted the site-specific hydrolysis of all three RNA targets. Upon digestion of the duplexes formed by aggregated RNA targets (**12**) and (**13**) and 5'-DPPZ modified AONs (**3**) and (**8**) the new cleavage site was revealed which was never observed with PZN-modified AONs.
5. Although target RNAs have various degrees of tertiary structure, the cleavage rates of the AON/RNA hybrids hydrolysis by RNase H are comparable, showing that the single-strand availability in these RNAs for duplex formation with AONs are very similar, although sequence specificities are non-identical in the 11mer and 17mers RNAs, and the rate of AON/RNA hybrid formation is always higher than the hydrolysis rate by RNase H.
6. Sensitivity of RNase H to AON modifications is very different at different sites of AONs. At the 3'-end, neither the steric bulk nor charge of the chromophore made any difference in the hydrolysis rate in contrast to the 5'- or interior modifications.
7. The 3'-modifications dramatically improve the stability of AONs towards the 3'-exonucleases which prolongs the life-time of the ligand in the cell media. Also, the lipophilic moieties conjugated to the AONs affect the bio-distribution properties of antisense oligonucleotides and could influence the fraction of the drug delivered to different tissues.
8. The improved affinity and RNase H hydrolysis rate promoted by tethering of chromophores permits the use of shorter antisense oligonucleotides, which has the advantage of simplified synthesis and may lead to a cost-effective solution to the development of AONs as therapeutic agents. Also, the reduction of the number of PS-linkages (by reducing the length of the thio-AONs) should lead to lower immune stimulation and toxicity.

4. Materials and methods

4.1. Materials

T4 polynucleotide kinase and *E. coli* RNase H (5 units/ μ L) and [γ -³²P]ATP were purchased from Amersham Pharmacia Biotech (Sweden), phosphodiesterase I from *Crotalus Adamanteus* venom was from SIGMA. All oligonucleotides

were synthesized using an Applied Biosystems 392 automated DNA/RNA synthesizer.

4.2. Synthesis, deprotection and purification of oligonucleotides

Synthesis and deprotection of the phenazine-tethered, dipyrrophenazine-tethered [DPPZ-Ru(phen)₂]²⁺-tethered and phenazinium-tethered⁴² oligodeoxynucleotides as well as RNA targets were performed as previously described.^{25,26,43} Phosphorothioates were synthesized using tetraethylthiuram disulfide in acetonitrile (from Perkin-Elmer) as sulfurizing reagent. All oligonucleotides were purified by 20% 7 M urea polyacrylamide gel electrophoresis, and they are found to be homogenous both by PAGE and RP-HPLC (C-18 column). MALDI-MS analysis: AON (2) [M-H]⁻ 2980.76; calcd 2980.8; AON (3) [M-H]⁻ 3257.83; calcd 3257.8; AON (4) [M-H]⁻ 3023.68; calcd 3023.6; AON (5) [M-H]⁻ 3257.87; calcd 3257.8; AON (7) [M-H]⁻ 3108.84; calcd 3108.2; AON (8) [M-H]⁻ 3385.74; calcd 3385.8; AON (9) [M-H]⁻ 3151.54; calcd 3151.6; AON (10) [M-H]⁻ 3385.86; calcd 3385.8.

4.3. UV Melting experiments

Determination of the T_m s of the AON/RNA hybrids and RNA/RNA duplexes was carried out in the same buffer as for RNase H degradation: 57 mM Tris-HCl (pH 7.5), 57 mM KCl, 1 mM MgCl₂ and 2 mM DTT. Absorbance was monitored at 260 nm in the temperature range from 3°C to 60°C using Lambda 40 UV spectrophotometer equipped with Peltier temperature programmer with the heating rate of 1°C per minute. Prior to the measurements samples (1:1 mixture of AON and RNA) were preannealed by heating to 80°C for 5 min followed by slow cooling till 3°C and 30 min equilibration at this temperature.

4.4. Thermodynamic calculations from the UV experiments

The thermodynamic parameters characterizing the helix-to-coil transition for the DNA/RNA hybrids were obtained from T_m measurements over the concentration range from 2 to 10 μM (total strands concentration). Values of $1/T_m$ were plotted versus $\ln(C_t/4)$ and ΔH° and ΔS° parameters were calculated from slope and intercept of fitted line³⁸: $1/T_m = (R/\Delta H^\circ) \ln(C_t/S) + \Delta S^\circ/\Delta H^\circ$, where S reflects the sequence symmetry of the self ($S=1$) or non-self-complementary strands ($S=4$).

4.5. CD Experiments

CD spectra were measured on a JASCO J41-A Spectropolarimeter from 320 to 220 nm in thermostated 0.2 mm path length cuvette. Buffer conditions were the same as for the UV and RNase H experiments: 57 mM Tris-HCl (pH 7.5), 57 mM KCl, 1 mM MgCl₂ and 2 mM DTT. The total strand concentration of 2 μM was used in the experiments with AON/RNA hybrids and 1 and 2.5 μM in the experiments with RNA targets. CD spectra of the AON/RNA hybrids were measured at 16°C. Melting transitions of the RNA targets were determined by recording CD spectra with 3°C intervals over the temperature range from 3°C

to 60°C. Ellipticities at 265 nm were plotted against temperature and the T_m values were obtained by fitting the sigmoidal curves with variable slopes using the GraphPad Prism software.

4.6. Thermodynamic calculations from the CD experiments

Thermodynamic parameters of duplex formation for each RNA target were extracted from the single temperature dependent CD curve using a calculation procedure described earlier.⁴⁴ In this procedure, equilibrium constants K for each temperature point were calculated as $K = f/2(1-f)^2 C_t$ where f is a fraction of duplex and C_t is the total strand concentration. A plot of $\ln K$ vs $1/T$ yielded the enthalpy, ΔH° , and entropy, ΔS° , from the slope and intercept, respectively: $\ln K = -\Delta H^\circ/T + \Delta S^\circ$.

4.7. ³²P Labelling of oligonucleotides

The oligoribonucleotides, oligodeoxyribonucleotides as well as phosphorothioates were 5'-end labelled with ³²P using T4 polynucleotide kinase, [γ -³²P]ATP and standard procedure. Labelled RNAs were purified by 20% denaturing PAGE and specific activities were measured using Beckman LS 3801 counter.

4.8. RNase H digestion assays

DNA/RNA hybrids (0.8 μM) consisting of 1:1 mixture of antisense oligonucleotide and target RNA (specific activity 50 000 cpm) were digested with 0.3 U of RNase H in 57 mM Tris-HCl (pH 7.5), 57 mM KCl, 1 mM MgCl₂ and 2 mM DTT at 21°C. Prior to the addition of the enzyme reaction components were preannealed in the reaction buffer by heating at 80°C for 5 min followed by 1.5 h of equilibration at 21°C. Total reaction volume was 26 μl. Aliquots (7 μl) were taken after 15 and 120 min and reaction was stopped by addition of the equal volume of 20 mM EDTA in 95% formamide. RNA cleavage products were resolved by 20% polyacrylamide denaturing gel electrophoresis and visualized by autoradiography. Quantitation of cleavage products was performed using a Molecular Dynamics PhosphorImager.

4.9. Nuclease degradation studies

Stability of the 3'-end modified phosphodiester oligonucleotides and phosphorothioate oligonucleotides as well as non modified DNA and thio-DNA towards 3'-exonucleases was tested using snake venom phosphodiesterase from *Crotalus adamanteus*. All reactions were performed at 3 μM DNA concentration (5'-end ³²P labeled with specific activity 50 000 cpm) in 56 mM Tris-HCl (pH 7.9) and 4.4 mM MgCl₂ at 22°C. Exonuclease concentration of 35 ng/μl was used for digestion of the phosphodiester oligonucleotides and 175 ng/μl for the phosphorothioate oligonucleotides. Aliquots were quenched by addition of the same volume of 20 mM EDTA in 95% formamide. Reaction progress was monitored by 20% 7 M urea PAGE and autoradiography. The half-life was determined as degradation of the full-length oligonucleotide to the $n-1$ and smaller fragments.

Acknowledgements

Thanks are due to the Swedish Board for Technical Development (NUTEK), the Swedish Natural Science Research Council (NFR) and the Swedish Research Council for Engineering Sciences (TFR) for generous financial support.

References

- Manoharan, M. *Biochim. Biophys. Acta* **1999**, *1489*, 117.
- Crum, C. *Nucleic Acids Res.* **1988**, *10*, 4569.
- Krieg, A.; Stein, C. *Antisense Res. Dev.* **1995**, *5*, 241.
- Lesnik, E. A.; Guinosso, C. J.; Kawasaki, A. M.; Sasmor, H.; Zounes, M.; Cummins, L. L.; Ecker, D. J.; Cook, P. D.; Freier, S. M. *Biochemistry* **1993**, *32*, 7832.
- Martin, P. *Helv. Chim. Acta* **1995**, *78*, 486.
- Kawasaki, A. M.; Casper, M. D.; Freier, S. M.; Lesnik, E. A.; Zounes, M. C.; Cummins, L. L.; Gonzalez, C.; Cook, P. D. *J. Med. Chem.* **1993**, *36*, 831.
- Wengel, J. *Acc. Chem. Res.* **1999**, *32*, 301.
- Ramasamy, K. S.; Zounes, M.; Gonzalez, C.; Freier, S. M.; Lesnik, E. A.; Cummins, L. L.; Griffeu, R. H.; Monia, B. P.; Cook, P. D. *Tetrahedron Lett.* **1994**, *2*, 215.
- Damha, M. J.; Wilds, C. J.; Noronha, A.; Brukner, I.; Borkow, G.; Arion, D.; Parniak, M. A. *J. Am. Chem. Soc.* **1998**, *120*, 12976.
- (a) Wang, G.; Middleton, P. J.; Lin, C.; Pietrzkowski, Z. *Bioorg. Med. Chem. Lett.* **1999**, *9*, 885. (b) Kanazaki, M.; Ueno, Y.; Shuto, S.; Matsuda, A. *J. Am. Chem. Soc.* **2000**, *122*, 2422.
- (a) Summerton, J. *Biochim. Biophys. Acta* **1999**, *1489*, 141. (b) Larsen, H. J.; Bentin, T.; Nielsen, P. E. *Biochim. Biophys. Acta* **1999**, *1489*, 159. (c) Gagnor, C.; Bertrand, J.-R.; Thenet, S.; Lemaitre, M.; Morvan, F.; Rayner, B.; Malvy, C.; Lebleu, B.; Imbach, J.-L.; Paoletti, C. *Nucleic Acids Res.* **1987**, *24*, 10419. (d) Hendrix, C.; Rosemeyer, H.; Bouvere, B. D.; Aerschot, A. V.; Seela, F.; Herdewijn, P. *Chem. Eur. J.* **1997**, *9*, 1513.
- (a) Stein, C. A.; Cheng, Y.-C. *Science* **1993**, *261*, 1004. (b) Cazenave, C.; Stein, C. A.; Loreau, N.; Thuong, N. T.; Neckers, L. M.; Subasinghe, C.; Helene, C.; Cohen, J. S.; Toulm, J.-J. *Nucleic Acids Res.* **1989**, *17*, 4255.
- Rait, V. K.; Shaw, B. R. *Antisense Nucleic Acid Drug Dev.* **1999**, *9*, 53.
- (a) Miller, P. S. *Oligodeoxynucleotides: Antisense Inhibitors of Gene Expression*, Cohen, J. S., Ed., CRC: Boca Raton, FL, 1989; pp 79. (b) Furdon, P. J.; Dominski, Z.; Kole, R. *Oligodeoxynucleotides: Antisense Inhibitors of Gene Expression. Nucleic Acids Res.* **1989**, *22*, 9193.
- Agrawal, S.; Mayrand, S. H.; Zamecnik, P. C.; Pederson, T. *Proc. Natl. Acad. Sci. USA* **1990**, *87*, 1401.
- Jones, R. J.; Lin, K.-Y.; Milligan, J. F.; Wadwani, S.; Matteucci, M. D. *J. Org. Chem.* **1993**, *58*, 2983.
- Morvan, F.; Sanghvi, Y. S.; Perbost, M.; Vasseur, J.-J.; Bellon, L. *J. Am. Chem. Soc.* **1996**, *118*, 255.
- Gryaznov, S. M. *Biochim. Biophys. Acta* **1999**, *1489*, 131.
- (a) Giles, R. V.; Tidd, D. M. *Nucleic Acids Res.* **1992**, *4*, 763. (b) Agrawal, S.; Jiang, Z.; Zhao, Q.; Shaw, D.; Cai, Q.; Roskey, A.; Channavajjala, L.; Saxinger, C.; Zhang, R. *Proc. Natl. Acad. Sci. USA* **1997**, *94*, 2620. (c) Agrawal, S. *Biochim. Biophys. Acta* **1999**, *1489*, 53.
- Gutierrez, A. J.; Matteucci, M. D.; Grant, D.; Matsumura, S.; Wagner, R. W.; Froehler, B. C. *Biochemistry* **1997**, *36*, 743.
- Flanagan, W. M.; Wolf, J. J.; Olson, P.; Grant, D.; Lin, K.-Y.; Wagner, R. W.; Matteucci, M. D. *Proc. Natl. Acad. Sci. USA* **1999**, *96*, 3513.
- Hélène, C.; Toulme, J.-J. *Biochim. Biophys. Acta* **1990**, *1049*, 99.
- Wagner, R. W.; Matteucci, M. D.; Grant, D.; Huang, T.; Froehler, B. C. *Nat. Biotechnol.* **1996**, *14*, 840.
- Puri, N.; Chattopadhyaya, J. *Nucleosides and Nucleotides* **1999**, *18*, 2785.
- Ossipov, D.; Zamaratski, E.; Chattopadhyaya, J. *Helv. Chim. Acta* **1999**, *82* (12), 2186–2200.
- Zamaratski, E.; Chattopadhyaya, J. *Tetrahedron* **1998**, *54* (28), 8183.
- Marky, L. A.; Breslauer, K. J. *Biopolymers* **1987**, *26*, 1601.
- Alen, F. S.; Gray, D. M.; Roberts, G. P.; Tinoco, I. *Biopolymers* **1972**, *11*, 853.
- Griffey, R. H.; Monia, B. P.; Cummins, L. L.; Freier, S.; Greig, M. J.; Guinosso, C. J.; Lesnik, E.; Manalili, S. M.; Mohan, V.; Owens, S.; Ross, B. R.; Sasmor, H.; Wancewicz, E.; Weiler, K.; Wheeler, P. D.; Cook, P. D. *J. Med. Chem.* **1996**, *39*, 5100.
- (a) Lima, W. F.; Mohan, V.; Crooke, S. T. *J. Biol. Chem.* **1997**, *272*, 18191. (b) Li, J.; Wartell, R. M. *Biochemistry* **1998**, *37*, 5154. (c) Puri, N.; Chattopadhyaya, J. *Tetrahedron* **1999**, *55* (5), 1505.
- Tinoco, I.; Sauer, K.; Wang, J. C. *Physical Chemistry: Principles and Applications in Biological Sciences*, Young, D., Cavanaugh, D., Eds., Prentice Hall: Upper Saddle River, NJ, 1995; pp 559–589.
- Davis, T. M.; McFail-Isom, L.; Keane, E.; Williams, L. D. *Biochemistry* **1998**, *37*, 6975.
- Ratmeyer, L.; Vinayak, R.; Zhong, Y. Y.; Zon, G.; Wilson, W. D. *Biochemistry* **1994**, *33*, 5298.
- Fedoroff, O. Yu.; Salazar, M.; Reid, B. R. *J. Mol. Biol.* **1993**, *233*, 509.
- Yu, D.; Kandimalla, E. R.; Roskey, A.; Zhao, Q.; Chen, L.; Chen, J.; Agrawal, S. *Bioorg. Med. Chem.* **2000**, *8*, 275.
- Crooke, S. T. *Therapeutic Applications of Oligonucleotides*, R.G. Landes Co.: Austin, TX, 1995.
- Temsamani, J.; Tang, J.-Y.; Padmapriya, A.; Kubert, M.; Agrawal, S. *Antisense Res. Dev.* **1993**, *3*, 277.
- Nicklin, P. L.; Ambler, J.; Mitchelson, A.; Bayley, D.; Phillips, J. A.; Craig, S. J.; Monia, B. P. *Proc. Natl. Acad. Sci. USA* **1997**, *16*, 1145.
- Vlassov, V. V.; Yakubov, L. A. *Oligonucleotides: Antisense Inhibitors of Gene Expression*, Cohen, J. S., Ed., Macmillan: London, 1989; pp 243.
- (a) Boutorin, A. S.; Guskova, L. V.; Ivanova, E. M.; Kobetz, N. D.; Zafytova, V. F.; Ryte, A. S.; Yurchenko, L. V.; Vlassov, V. V. *FEBS Lett.* **1989**, *254*, 129. (b) Ryte, A. S.; Karamyshev, V. N.; Nechaeva, M. N.; Guskova, Z. V.; Ivanova, E. M.; Zarytova, V. F.; Vlassov, V. V. *FEBS Lett.* **1992**, *299*, 124.
- Vorobjev, P. E.; Zarytova, V. F.; Borona, G. M. *Nucleosides and Nucleotides* **1999**, *18*, 2745.
- Lokhov, S. G.; Podyminogin, M. A.; Sergeev, D. S.; Silnikov, V. N.; Kutyavin, I. V.; Shishkin, G. V.; Zarytova, V. P. *Bioconjug. Chem.* **1992**, *3* (5), 414.
- Ossipov, D.; Chattopadhyaya, J. manuscript in preparation.
- Albergo, D. P.; Marky, L. A.; Breslauer, K. J.; Turner, D. H. *Biochemistry* **1981**, *20* (6), 1409.